Prepared for submission to JCAP

arXiv:1407.1632v2 [astro-ph.CO] 8 Sep 2014

Cosmic slowing down of acceleration for several dark energy parametrizations

Juan Magaña[a] **Víctor H. Cárdenas**[a] **Verónica Motta**[a]

[a]Instituto de Física y Astronomía, Facultad de Ciencias, Universidad de Valparaíso, Avda. Gran Bretaña 1111, Valparaíso, Chile.

E-mail: juan.magana@uv.cl, victor.cardenas@uv.cl, veronica.motta@uv.cl

Abstract. We further investigate slowing down of acceleration of the universe scenario for five parametrizations of the equation of state of dark energy using four sets of Type Ia supernovae data. In a maximal probability analysis we also use the baryon acoustic oscillation and cosmic microwave background observations. We found the low redshift transition of the deceleration parameter appears, independently of the parametrization, using supernovae data alone except for the Union 2.1 sample. This feature disappears once we combine the Type Ia supernovae data with high redshift data. We conclude that the rapid variation of the deceleration parameter is independent of the parametrization. We also found more evidence for a tension among the supernovae samples, as well as for the low and high redshift data.

Keywords: dark energy, Cosmology

Contents

1 Introduction **1**

2 The cosmological framework **2**

3 Parametrizations of the dark energy equation of state **2**
- 3.1 Jassal-Bagla-Padmanabhan parametrization 3
- 3.2 Feng-Shen-Li-Li parametrization 3
- 3.3 Polynomial parametrization 3
- 3.4 Barbosa-Alcaniz parametrization 4

4 Cosmological constraints from observational data **4**

5 Discussion and Conclusions **8**

1 Introduction

The observations from Type Ia supernova (SNIa) were the first clear evidence of the accelerated expansion of the Universe [1, 2]. The hypothesis of an expanding universe is currently supported by a wide range of large-scale measurements [3–5]. To explain this acceleration within general relativity, it is necessary to introduce an exotic component, named dark energy (DE). Current observations point towards a cosmological constant Λ [6–8]; nevertheless, it could be necessary to consider dynamical DE models where the equation of state (EoS) parameter, w, is a function of the scale factor a (or redshift z), i.e. $w = P/\rho = w(a)$, where P and ρ are the pressure and energy density of DE respectively [9–12]. One popular ansatz for this dynamical EoS is the Chevallier-Polarski-Linder (CPL) parametrization [13, 14] given by $w(a) = w_0 + (1-a)w_1$, where w_0 is the present value of the EoS and w_1 is the derivative with respect to scale factor. Recently, [15] found a cosmic slowing down of the acceleration at low redshifts using the CPL model with the Constitution SNIa sample in combination with baryon acoustic oscillation (BAO) data. Nevertheless, this apparent behavior disappears when the cosmic microwave background (CMB) data are added in the analysis, indicating a tension between low and high redshift measurements. Similarly, using the Union2 SNIa set, [16] it was found the same behavior at low redshift. The authors of [17] found the tension between the sets at low redshifts and at high redshifts can be ameliorated incorporating a curvature term as a free parameter in the analysis.

The slowing down scenario using only supernovas can be considered a sort of an artifact from the data. However, recent studies have been able to demonstrate the same trend using using 42 measurements of gas mass fraction in galaxy clusters [18]. They found the same trend as using SNIa, i.e. the acceleration of the universe has already reached its maximum at $z \sim 0.2$ and is currently moving towards a decelerating phase, in agreement with previous works. At this point it would be interesting to know if this feature is only an artifact of the CPL parametrization.

In this paper we study the cosmic slowing down of the acceleration at low redshifts using four SNIa sets: Constitution, Union 2, Union 2.1, and LOSS-Union, together with five

parametrizations of the EoS of dark energy. We also consider the constraints from BAO and CMB from the Wilkinson Microwave Anisotropy Probe (WMAP) 9-yr observations.

The paper is organized as follows: in the next section we introduce the cosmological framework for a flat universe case. In section §3 we present the dynamical models of dark energy. We describe in §4 the SNIa data used to constrain the parameters of the models and present our results. Finally, we discuss the results and present our conclusions in section §5

2 The cosmological framework

We consider a flat Friedmann-Lemaître-Robertson-Walker (FLRW) universe whose DE has a dynamical EoS $w(z)$. The dimensionless Hubble parameter $E(z)$ for this universe is given by

$$E^2(z) = H^2(z)/H_0^2 = \Omega_m(1+z)^3 + \Omega_r(1+z)^4 + \Omega_{de}X(z), \tag{2.1}$$

where Ω_m is the density parameter for matter. The density parameter for radiation is $\Omega_r = 2.469 \times 10^{-5}h^{-2}(1+0.2271N_{eff})$, where $h = H_0/100\,\mathrm{kms}^{-1}\mathrm{Mpc}^{-1}$ and the number of relativistic species is set to $N_{eff} = 3.04$ [19]. The density parameter for DE is written as $\Omega_{de} = 1 - \Omega_m - \Omega_r$ and the function $X(z)$ reads as

$$X(z) = \frac{\rho_{de}(z)}{\rho_{de}(0)} = \exp\left(3\int_0^z \frac{1+w(z)}{1+z}\mathrm{dz}\right), \tag{2.2}$$

where $\rho_{de}(z)$ is the energy density of DE at redshift z, and $\rho_{de}(0)$ its present value. The comoving distance from the observer to redshift z is given by

$$r(z) = \frac{c}{H_0}\int_0^z \frac{dz'}{E(z')}. \tag{2.3}$$

The deceleration parameter *q(z)* is defined as

$$q(z) = -\frac{\ddot{a}(z)a(z)}{\dot{a}^2(z)}, \tag{2.4}$$

where a is the scale factor of the Universe. Using eq. (2.1), this expression can be rewritten as

$$q(z) = -\frac{(1+z)}{E(z)}\frac{dE(z)}{dz} - 1. \tag{2.5}$$

In the following section, we study five different parametrizations of $w(z)$ and for each one we shall use expression (2.5) to reconstruct the deceleration parameter.

3 Parametrizations of the dark energy equation of state

Because we do not known what physics is behind the DE, one way to explore models going beyond the cosmological constant is by using an explicit parametrization for the EoS parameter $w(z)$. Actually, the apparent cosmic slowing down of acceleration was found first using an explicit parametrization of $w(z)$. This low redshift feature of the reconstructed $q(z)$, remains after using different data sets by applying the CPL parametrization [15, 18]. In the [20], the author adopted a different approach focusing his study not in a $w(z)$ trial function, but in a simple (blind analysis) interpolation for the DE density $X(z)$. However,

he found the same low redshift transition for the reconstructed $q(z)$. This means that both are valid complementary methods which enable us to explore evolution in the DE density, and consequently, the cosmic acceleration.

In this work, although we do not expect that a phenomenological specific parametrization for $w(z)$ will reproduce the eventual real behavior of $q(z)$, we investigate through several parametrizations of the DE EoS whether the cosmic slowing down of acceleration is a real feature of the Universe at low redshifts. We choose parametrizations with two independent free parameters, thus allowing for direct statistical model comparisons. In the following we introduce the parametrizations to be tested by cosmological data.

3.1 Jassal-Bagla-Padmanabhan parametrization

Jassal-Bagla-Padmanabhan (JBP) [21, 22] propose an EoS of DE as function of redshift in the following way

$$w(z) = w_0 + w_1 \frac{z}{(1+z)^2}, \tag{3.1}$$

where $w_0 = w(0)$, $w_1 = w'(0)$, and $w(\infty) = w_0$. In addition, the EoS parameter has the same value at present and early epochs and performs a rapid variation around $z = 1$ with amplitude $w_0 + w_1/4$. For the JBP parametrization (3.1), the function (2.2) reads as

$$X(z) = (1+z)^{3(1+w_0)} \exp\left(\frac{3}{2}\frac{w_1 z^2}{(1+z)^2}\right), \tag{3.2}$$

and $E(z)$ is completely determined.

3.2 Feng-Shen-Li-Li parametrization

Another interesting parametrization was proposed by Feng, Shen, Li and Li (FSLL) [23] to overcome the divergence of the CPL model when $z \to -1$. They propose the two following relations:

$$\begin{aligned} \text{FSLL I}: \quad w(z) &= w_0 + w_1 \frac{z}{1+z^2}, \\ \text{FSLL II}: \quad w(z) &= w_0 + w_1 \frac{z^2}{1+z^2}, \end{aligned} \tag{3.3}$$

where for both models $w_0 = w(0)$ and $w_1 = w'(0)$. For FSLL I, $w(\infty) = w_0$ and at low redshift it reduces to the linear form $w(z) \approx w_0 + w_1 z$, while for FSLL II $w(\infty) = w_0 + w_1$ and at low redshifts it yields $w(z) \approx w_0 + w_1 z^2$. For the parametrizations (3.3), the functions (2.2) are given by

$$X(z)_{\pm} = (1+z)^{3(1+w_0)} \exp\left[\pm\frac{3w_1}{2}\arctan(z)\right] \left(1+z^2\right)^{3w_1/4} (1+z)^{\mp 3w_1/2}, \tag{3.4}$$

where X_+ and X_- correspond to FSLL I and FSLL II respectively.

3.3 Polynomial parametrization

A generalization of the CPL model consists in an expansion in powers of $(1+z)$ [24]. One of these polynomial parametrizations was proposed by Sendra and Lazkoz (SL) [25]

$$w(z) = -1 + c_1\left(\frac{1+2z}{1+z}\right) + c_2\left(\frac{1+2z}{1+z}\right)^2, \tag{3.5}$$

where $c_1 = (16w_0 - 9w_{0.5} + 7)/4$, $c_2 = -3w_0 + (9w_{0.5} - 3)/4$, w_0 and $w_{0.5}$ are the values of the equation of state at $z = 0$ and $z = 0.5$ respectively. This description of the EoS in terms of $w_{0.5}$ improved the situation of the CPL model, which suffers from a significant correlation between the parameters w_0 and w_1 [26]. The proposed function is:

$$X(z) = (1+z)^{3(1-8w_0+9w_1)/2} \exp\left[\frac{3z(w_0(52z+40) - 9w_1(5z+4) + 7z + 4)}{8(1+z)^2}\right]. \tag{3.6}$$

Notice the ΛCDM model is recovered for $w_0 = w_{0.5} = -1$.

3.4 Barbosa-Alcaniz parametrization

We also consider the Barbosa-Alcaniz parametrization [27], where:

$$w(z) = w_0 + w_1 \frac{z(1+z)}{1+z^2}, \tag{3.7}$$

where $w_0 = w(0)$, $w_1 = w'(0)$, $w(\infty) = w_0 + w_1$, and at low redshift it reduces to the linear form $w(z) \approx w_0 + w_1 z$. This ansatz is a well behaved function of the redshift z over the range $z \in [-1, \infty)$. The DE density in this case evolves as

$$X(z) = (1+z)^{3(1+w_0)}(1+z^2)^{3w_1/2}. \tag{3.8}$$

As a closing for this section, we have to mention that an important condition that a given parametrization must fulfill, is that the DE density has to be lower that the matter energy density in the past. This is easily checked using the explicit expressions we have derived, finding that all of our best fit functions satisfies this requirement.

4 Cosmological constraints from observational data

The maximal probability analysis we perform to constrain the parameters of the different parametrizations considers cosmological observations at different redshifts: Type Ia supernovae data, the acoustic peaks of BAO and the WMAP 9-yr distance posterior. In all our analysis, we assume a flat geometry, and a fixed reduced Hubble constant $h = 0.697$ [3], thus leaving Ω_m, w_o, and w_1 ($w_{0.5}$ for the SL model) as the only free parameters of the problem. For the supernova data we use the Constitution (C) set consisting of 397 SNIa points [28] covering a redshift range $0.015 < z < 1.551$, Union 2 (U2) consisting in 557 points in the redshift range $0.511 < z < 1.12$ [29], and Union 2.1 (U21) which consists of 580 points in the redshift range $0.015 < z < 1.41$ [30]. We also use the sample presented by [31] consisting in 586 SNIa in the redshift range $0.01 - 1.4$ which considers 91 points of the Lick Observatory Supernova Search (LOSS) sample [32]. Hereafter, we refer to it as LOSS-Union (LU) set.

The SNIa samples give the distance modulus as a function of redshift $\mu_{obs}(z)$ and its error σ_μ. Theoretically, the distance modulus is computed as

$$\mu(z) = 5\log_{10}[d_L(z)/\mathtt{Mpc}] + 25, \tag{4.1}$$

which is a function of the cosmology through the luminosity distance (measured in Mpc)

$$d_L(z) = (1+z)r(z), \tag{4.2}$$

valid for a flat universe with $r(z)$ given by Eq. (2.3). We fit the SNIa with the cosmological model by minimizing the χ^2 value defined as

$$\chi^2_{SNIa} = \sum_{i=1}^{N} \frac{[\mu(z_i) - \mu_{obs}(z_i)]^2}{\sigma^2_{\mu_i}}. \tag{4.3}$$

We also consider the data from BAO and CMB. The BAO measurements considered in our analysis are the following: three acoustic parameter measurements at $z = 0.44$, 0.6, and 0.73 from the WiggleZ experiment[33], two BAO distance measurements at $z = 0.2$, and 0.35 from the Sloan Digital Sky Survey Data Release 7 (SDSS DR7) [34], and one data point at $z = 0.106$ from the Six-degree-Field Galaxy Survey (6dFGS) [35]. Thus, the total χ^2 for all the BAO data sets can be written as $\chi^2_{BAO} = \chi^2_{WiggleZ} + \chi^2_{SDSS} + \chi^2_{6dFGS}$ (see [18] for more details to construct χ^2_{BAO}). The CMB information considered is derived from the 9 years WMAP data [3]. In our analysis we compare the measurements of the acoustic scale, the shift parameter and the redshift of decoupling with the theoretical ones (see [18] for details to construct χ^2_{CMB}). We constrain the cosmological parameters for two cases: using only the Type Ia supernovae data, where the $\chi^2_{Tot} = \chi^2_{SNIa}$; and using all data (SNIa+BAO+CMB), where $\chi^2_{Tot} = \chi^2_{SNIa} + \chi^2_{BAO} + \chi^2_{CMB}$. We minimize these χ^2_{Tot} functions with respect to the parameters $\{\Omega_m, w_0, w_1(w_{0.5})\}$ to compute the best estimated values and their errors.

Our results from the Bayesian analysis for the models are given in Table 1. In Fig. 1 we show the evolution of the deceleration parameter as function of redshift for the JBP parametrization using the best fit values for these data sets. Notice that using the C set

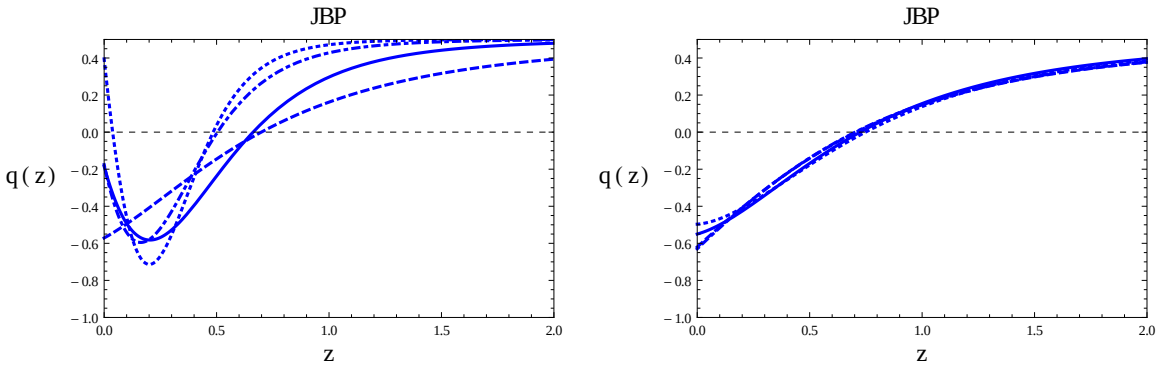

Figure 1. Evolution of the deceleration parameter $q(z)$ vs z for the JBP parametrization. The left panel shows the reconstructed $q(z)$ using the best fit obtained from Constitution (dotted line), Union 2 (dot-dashed line), Union 2.1 (dashed line) and LOSS-Union (solid line) samples. The right panel shows the reconstructed $q(z)$ using the best fit obtained from C+BAO+CMB (dotted line), U2+BAO+CMB (dotted-dash line), U21+BAO+CMB (dashed line) and LU+BAO+CMB (solid line). Notice the cosmic slowing down of the acceleration at $z \sim 0.2$ for the SNIa sets excepts for Union2.1 sample. This feature disappears when adding BAO and CMB data.

the Universe pass through a maximum of acceleration at $z \sim 0.2$ and now evolves towards a decelerating phase in the near future. The same slowing down of acceleration occurs using U2 (at $z \sim 0.17$), and LU (at $z \sim 0.2$) sets. This feature is preserved when propagating the error at 1σ in the best fit parameter. Therefore, there is a statistically significant evidence of the cosmic slowing down of the acceleration at low redshifts. Nevertheless this behavior does not occur using the U2.1 data. When adding the information from BAO and CMB data, the Universe has a transition from a decelerated phase to an accelerated phase at $z \sim 0.7$

(for all SNIa samples). Our analysis strongly suggests a tension between low-redshifts and high-redshifts measurements. This results is in agreement with the previous works using SNIa data and information from galaxy clusters [15–18].

In Fig. 2 we show the reconstructed $q(z)$ as function of z for the FSLL I model. Notice that the slowing down of the acceleration occurs at $z \sim 0.22$, $z \sim 0.18$, $z \sim 0.25$ using C, U2 an LU samples respectively. For the FSLL II parametrization, the cosmic deceleration occurs at $z \sim 0.27$, $z \sim 0.25$, $z \sim 0.3$ using the same SNIa sets respectively (Figure 3). Nevertheless $q(z)$ has another transition at $z \sim 0.07$ for U2 and LU sets, and the Universe begins an accelerated phase. However, this oscillating behavior is not statistically significant when propagating the error at 1σ in the best fit parameters. Using the U2.1 SNIa sample there is no evidence for the deceleration of the Universe at low redshift. As is shown in Figure 4 the slowing down of the acceleration for the SL $w(z)$ function occurs at $z \sim 0.22$, $z \sim 0.18$, $z \sim 0.23$ using C, U2 and LU samples respectively. Finally, in Fig. 5 we show that the Universe has a maximum of acceleration and it begins to decelerate at $z \sim 0.24$, $z \sim 0.19$, $z \sim 0.25$ using the same SNIa samples respectively.

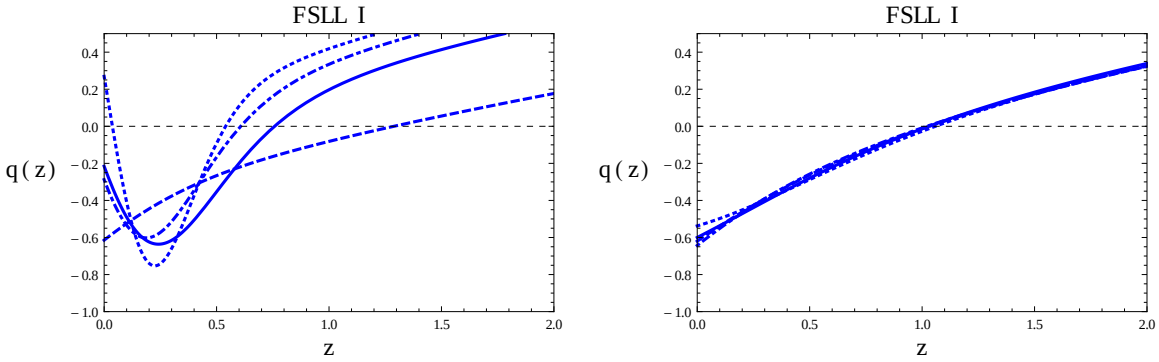

Figure 2. We show the slope of the $q(z)$ as in Fig. 1 for the FSLL I parametrization.

Therefore, our analysis shows significant evidence for a cosmic slowing down of the acceleration at low redshifts for dynamical DE models with EoS varying with redshift using Constitution, Union 2 and LOSS-Union SNIa sets. Interestingly, this feature disappears when using the Union 2.1 sample, which suggests an important tension between this particular data set and the other SNIa samples. Moreover, when the analysis is performed using the combination of SNIa data with the BAO and CMB observations, the scenario of the deceleration of the Universe's expansion at low redshift disappears. Actually, we obtain $w(0) \approx -1$ at 1σ for all parametrizations in agreement with a cosmological constant. Moreover, we found that the Universe has a transition from a decelerated phase to an accelerated phase at $z \sim 1$, $z \sim 0.7$, $z \sim 0.75$ and $z \sim 0.7$ for the FSLL I, FSLL II, SL, and BA parametrizations respectively. Therefore, we found more evidence pointing out a tension between the low and high redshift data.

Our results are in agreement with previous work [15, 17, 18], showing that even with more new data points, the tension between the low and hight redshift observational probes remains. One of the main result of this work is to remove the uncertainty about the effect of the parametrization of $w(z)$ on the results and final conclusions. Recently [20] found a connection between this low redshift transition of $q(z)$ with the DE density decreasing with increasing redshift. Therefore, it would be important to check such a behavior. In Figure 6 we show the slope of the $X(z)$ function for all the five parametrizations using the best

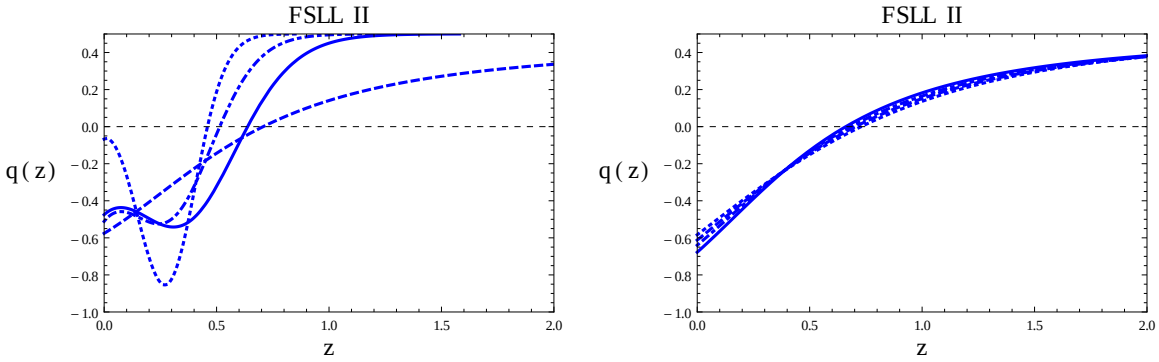

Figure 3. We show the slope of the $q(z)$ as in Fig. 1 for the FSLL II parametrization.

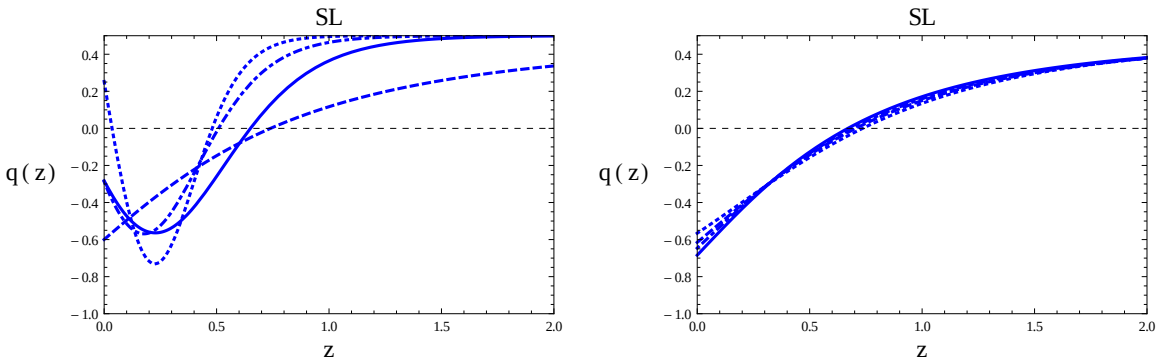

Figure 4. Idem as Fig. 1 for the SL parametrization.

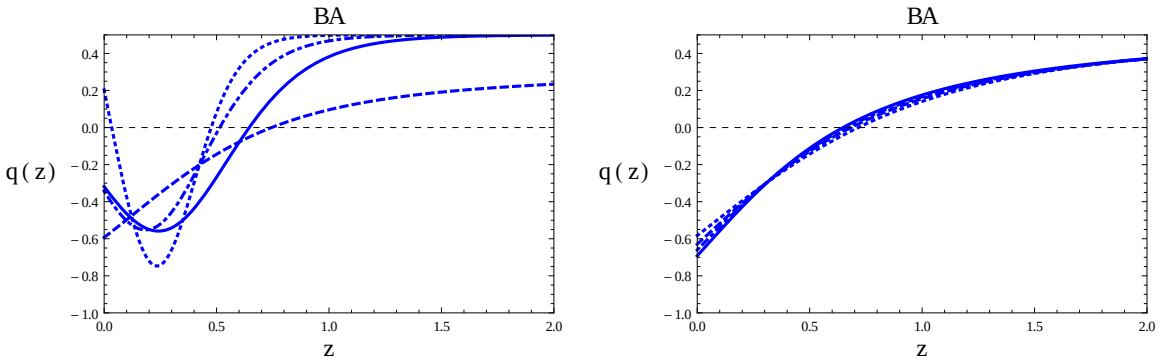

Figure 5. We show the slope of the $q(z)$ as in Fig. 1 for the BA parametrization.

fit parameters estimated from the LOSS-Union sample. The low redshift data suggest the DE density is in fact increasing with time. This same behavior occurs using the constraints derived from the other Type Ia supernovae data. As it was mentioned in [20] this particular results is in agreement with the recent BAO DR11 measurements [36] where a tension between BAO data and CMB was informed. This tension reveals that, in order to accommodate these new data assuming a flat universe with dark matter and DE, we have to assume the DE

density decreases with increasing redshift, and it reaches a negative value at $z \simeq 2.4$,

$$\frac{\rho_{de}(z=2.34)}{\rho_{de}(z=0)} = -1.2 \pm 0.8, \tag{4.4}$$

in agreement with what we have found in this work. Similar conclusions are obtained in [46] based on the same data from BAO.

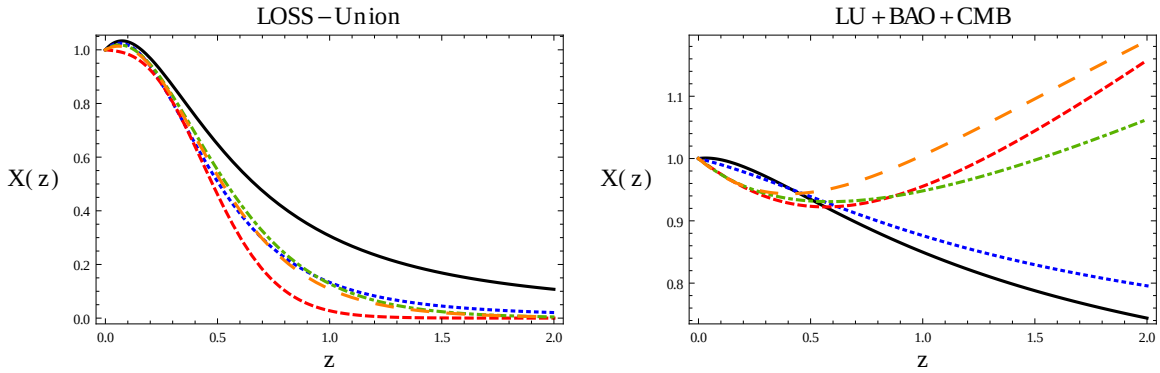

Figure 6. Evolution of the function $X(z)$ vs z for all parametrizations. The left panel shows the reconstructed $X(z)$ using the best fit obtained from LOSS-Union for the JBP (solid line), FSLL I (dotted line), FSLL II (dashed), SL (dot-dashed) and, BA (long dashed) parametrizations. The right panel shows the reconstructed $X(z)$ using the best fit obtained from LOSS-Union+BAO+CMB for the five parametrizations. Notice the low redshift data suggest the DE density is in fact increasing with time. This same behavior occurs using the constraints derived from the other Type Ia supernovae data.

To discern which model is the preferred one by observations we only compare the χ^2_{min}, given in Table 1, among data sets. Notice there is no significant differences among these values for the parametrizations and, it is difficult to distinguish which model is the favored by the data. Therefore, any parametrization could be a plausible model of dynamical dark energy.

5 Discussion and Conclusions

In this paper, we have studied five alternative models for dark energy with an equation of state varying with redshift. We put constraints on the parameters for these parametrizations using four different SNIa samples. We reconstructed the cosmological evolution of the deceleration parameter, and found that using the best fit obtained with Constitution, Union 2 and LOSS-Union samples, the Universe reaches a maximum of acceleration at low redshift ($z \sim 0.25$), then it begins to decelerate for all parametrizations like CPL model. This is certainly a surprise because although models of the type wCDM with w =constant, using the same data, prefers a value $w < -1$ today [3, 4, 37], this work reveals that allowing a variation of $w(z)$ in any of the five parametrizations studied, implies the deceleration parameter has already reached its maximum and its evolving towards lower acceleration regimes. Nevertheless, this cosmic slowing down of the acceleration disappears using the constraints derived from the Union 2.1 SNIa set. This suggests a tension among the different SNIa compilations. This tension is very intriguing for Union 2 and Union 2.1 because they differ only in 24 data points and in the lightcurve fitter SALT for Union 2 and its improved version SALT2 for Union 2.1.

Similar tension between these Union 2.1 and Union 2 as well as other recent SNIa samples was also found by [37–39]. Additionally, Union 2.1 and LOSS-Union compilations are very similar and both of them use the lightcurve fitter SALT2 trained on data from low redshifts SNIa. However, they predict a reconstructed deceleration parameter considerably different. Therefore, we conclude the cosmic slowing down of the acceleration does not depend on the parametrization of the equation of state of dark energy and it could be due to several factors. For instance, systematic errors in the measurements from SNIa (such as peculiar motions [40, 41]), the presence of a Hubble bubble, anisotropic cosmological models, to mention some of them (see [18] for a discussion about this point). As was also discussed in [20], this low redshift transition of $q(z)$ was first found by the authors in [42], in the context of a Lemaitre-Tolman-Bondi inhomogeneous models. In that work, and also in recent ones ([43, 44]), the authors derived an effective deceleration parameter for void models, indicating that such a behavior of $q(z)$ may be considered as a signature for the existence of voids.Nevertheless, these results is in contrast with those obtained when a $q(z)$ parametrization is considered [45].

On the other hand, when adding the BAO and CMB measurements, the cosmic slowing down of the acceleration disappears for all parametrizations and they could mimic the cosmological constant at the present epoch. Therefore, we also confirmed a tension between the cosmological constraints obtained from low and high redshift data.

In agreement with the results of the recent BAO DR11 measurements [36] – where a tension between low to high redshift observational probes was detected – and also from the study in [20] – where the low redshift transition of $q(z)$ was demonstrated to be linked with a DE density that decrease with increasing redshift – we have also found evidence for DE density evolution. In fact, using the best fit parameters found for each parametrization, we can directly plot the DE density expressions (3.2), (3.4), (3.6) and (3.8), obtaining for each case the same result found first in [20]: the data suggest the DE density is increasing with epoch. The astonishing agreement between our approach based on using low redshift data (as SNIa, f_{gas}, and others) with the result obtained from BAO measurements [36], make a strong case for DE evolution, as it was recently highlighted in [46].

Acknowledgments

We thank the anonymous referee for thoughtful suggestions. We wish to acknowledge useful discussion with Diego Pavón and Gael Foëx. J.M. acknowledges support from ESO Comité Mixto, and Gemini 32130024. V.M. acknowledges support from FONDECYT 1120741, and ECOS-CONICYT C12U02. V.C. acknowledges support from FONDECYT Grant 1110230 and DIUV 13/2009,

References

[1] A. G. Riess *et al.*, *Observational evidence from supernovae for an accelerating universe and a cosmological constant*, Astron. J. **116** (1998) 1009, [astro-ph/9805201].

[2] S. Perlmutter *et al.*, *Measurements of Omega and Lambda from 42 high redshift supernovae*, Astrophys. J. **517** (1999) 565, [astro-ph/9812133].

[3] G. Hinshaw, D. Larson, E. Komatsu, D. N. Spergel, C. L. Bennett, J. Dunkley, M. R. Nolta and M. Halpern *et al.* [WMAP Collaboration], *Nine-Year Wilkinson Microwave Anisotropy Probe (WMAP) Observations: Cosmological Parameter Results*, Astrophys. J. Suppl. 208 (2013), 19, [arXiv:1212.5226].

[4] P. A. R. Ade *et al.*, *Planck 2013 results. XVI. Cosmological parameters*, 2013, [arXiv:1303.5076].

[5] T. M. Davis, *Cosmological constraints on dark energy*, Gen. Rel. Grav. 46 (2014) arXiv:1404.7266 [astro-ph.CO].

[6] P. Serra *et al.*, *No evidence for dark energy dynamics from a global analysis of cosmological data*, Phys. Rev. D. 80 (2009) 121302, [arXiv:0908.3186].

[7] R. Nair, J. Sanjay, *Is dark energy evolving?*, JCAP 02 (2013) 049, [arXiv:1212.6644].

[8] S. Postnikov, M. G. Dainotti, X. Hernandez and S. Capozziello, *Nonparametric Study of the Evolution of the Cosmological Equation of State with SNeIa, BAO, and High-redshift GRBs*, Astrophys. J. **783** (2014) 126 [arXiv:1401.2939 [astro-ph.CO]].

[9] C. Wetterich, *Cosmology and the Fate of Dilatation Symmetry*, Nucl. Phys. B **302** (1988) 668.

[10] S. Weinberg, *The cosmological constant problem*, Rev. Mod. Phys. 61 (1989) 1.

[11] E. J. Copeland, M. Sami, S. Tsujikawa, *Dynamics of dark energy*, Int. J. Mod. Phys. D 15 (2006), 1753, [arXiv:hep-th/0603057].

[12] J. Alberto Vazquez, M. Bridges, M. P. Hobson and A. N. Lasenby, *Reconstruction of the Dark Energy equation of state*, JCAP **1209** (2012) 020 [arXiv:1205.0847 [astro-ph.CO]].

[13] M. Chevallier, D. Polarski, *Accelerating Universes with Scaling Dark Matter*, Int. J. Mod. Phys. D , 10 (2001), 213, [gr-qc/0009008].

[14] E. V. Linder, *Mapping the Dark Energy Equation of State*, Phys. Rev. Lett. , 90 (2003), 091301, [astro-ph/0311403].

[15] A. Shafieloo, V. Sahni and A. A. Starobinsky, *Is cosmic acceleration slowing down?*, Phys. Rev. D. 80 (2009), 101301, [arXiv:0903.5141].

[16] Z. Li, P. Wu, H. Yu, *Examining the cosmic acceleration with the latest Union2 supernova data* Phys. Lett. B 695 (2011) 1, arXiv:1011.1982 [gr-qc].

[17] V.H. Cárdenas, M. Rivera, *The role of curvature in the slowing down acceleration scenario*, Phys. Lett. B , 710 (2012), 251, [arXiv:1203.0984].

[18] V.H. Cárdenas, C. Bernal, A. Bonilla, *Cosmic slowing down of acceleration using f_{gas}*, Mon. Non. Roy. Astron. Soc. , 433 (2013), 3534, [arXiv:1306.0779].

[19] E. Komatsu *et al.* [WMAP Collaboration], *Seven-Year Wilkinson Microwave Anisotropy Probe (WMAP) Observations: Cosmological Interpretation*, Astrophys. J. Suppl. **192** (2011) 18 [arXiv:1001.4538 [astro-ph.CO]].

[20] V. H. Cardenas, *Exploring dark energy density evolution in light of recent data*, 2014, arXiv:1405.5116 [astro-ph.CO].

[21] H. K. Jassal, J. S. Bagla and T. Padmanabhan, *WMAP constraints on low redshift evolution of dark energy*, Mon. Not. Roy. Astron. Soc. **356** (2005) L11 [astro-ph/0404378].

[22] H. K. Jassal, J. S. Bagla and T. Padmanabhan, *Observational constraints on low redshift evolution of dark energy: How consistent are different observations?*, Phys. Rev. D **72** (2005) 103503 [astro-ph/0506748].

[23] C. -J. Feng, X. -Y. Shen, P. Li and X. -Z. Li, *A New Class of Parametrization for Dark Energy without Divergence*, JCAP **1209** (2012) 023 [arXiv:1206.0063 [astro-ph.CO]].

[24] J. Weller and A. Albrecht, *Future supernovae observations as a probe of dark energy*, Phys. Rev. D **65** (2002) 103512 [astro-ph/0106079].

[25] I. Sendra and R. Lazkoz, *SN and BAO constraints on (new) polynomial dark energy parametrizations: current results and forecasts*, Mon. Not. Roy. Astron. Soc. **422** (2012) 776 [arXiv:1105.4943 [astro-ph.CO]].

[26] Y. Wang, *Figure of Merit for Dark Energy Constraints from Current Observational Data*, Phys. Rev. D **77** (2008) 123525 [arXiv:0803.4295 [astro-ph]].

[27] E. M. Barboza, Jr. and J. S. Alcaniz, *A parametric model for dark energy*, Phys. Lett. B **666** (2008) 415, [arXiv:0805.1713 [astro-ph]].

[28] M. Hicken et al., *Improved Dark Energy Constraints from 100 New CfA Supernova Type Ia Light Curves*, Astrophys. J. **700** (2009) 1097 [arXiv:0901.4804 [astro-ph.CO]].

[29] R. Amanullah *et al.*, *Spectra and Light Curves of Six Type Ia Supernovae at 0.511 ¡ z ¡ 1.12 and the Union2 Compilation*, Astrophys. J. **716** (2010) 712 [arXiv:1004.1711 [astro-ph.CO]].

[30] N. Susuki *et al.*, *The Hubble Space Telescope Cluster Supernova Survey. V. Improving the Dark-energy Constraints above $z > 1$ and Building an Early-type-hosted Supernova Sample* Astrophys. J. **746** (2012) 85 [arXiv:1105.3470].

[31] M. Ganeshalingam, W. Li and A. V. Filippenko, *Constraints on dark energy with the LOSS SN Ia sample*, Mon. Not. Roy. Astron. Soc. **433** (2013) 2240 arXiv:1307.0824 [astro-ph.CO].

[32] M. Ganeshalingam *et al.*, *Results of the Lick Observatory Supernova Search Follow-up Photometry Program: BVRI Light Curves of 165 Type Ia Supernovae*, Astrophys. J. Supp. **190** (2010) 418.

[33] C. Blake, E. Kazin, F. Beutler, T. Davis, D. Parkinson, S. Brough, M. Colless and C. Contreras *et al.*, *The WiggleZ Dark Energy Survey: mapping the distance-redshift relation with baryon acoustic oscillations*, Mon. Not. Roy. Astron. Soc. **418** (2011) 1707 [arXiv:1108.2635 [astro-ph.CO]].

[34] W. J. Percival *et al.*, *Baryon Acoustic Oscillations in the Sloan Digital Sky Survey Data Release 7Galaxy Sample*, 2010, Mon. Not. Roy. Astron. Soc. 401 (2010), 2148, [arXiv:0907.1660].

[35] F. Beutler, C. Blake, M. Colless, D. H. Jones, L. Staveley-Smith, L. Campbell, Q. Parker and W. Saunders *et al.*, *The 6dF Galaxy Survey: Baryon Acoustic Oscillations and the Local Hubble Constant*, Mon. Not. Roy. Astron. Soc. **416** (2011) 3017 [arXiv:1106.3366 [astro-ph.CO]].

[36] T. Delubac *et al.* [BOSS Collaboration], *Baryon Acoustic Oscillations in the Ly_α forest of BOSS DR11 quasars*, arXiv:1404.1801 [astro-ph.CO].

[37] D. L. Shafer and D. Huterer, *Chasing the phantom: A closer look at Type Ia supernovae and the dark energy equation of state*, Phys. Rev. D **89** (2014) 063510 [arXiv:1312.1688 [astro-ph.CO]].

[38] J.-F. Zhang, Y.-H. Li, X. Zhang, *A global fit study on the new agegraphic dark energy model*, Eur. Phys. J. C., 73 (2013) 2280, [arXiv:1212.0300].

[39] X. Yang, F. Y. Wang, Z. Chu, *Searching for a preferred direction with Union2.1 data*, Mon. Non. Roy. Astron. Soc. , 437 (2014) 1840, [arXiv:1310.5211].

[40] L. Hui and P. B. Greene, *Correlated Fluctuations in Luminosity Distance and the (Surprising) Importance of Peculiar Motion in Supernova Surveys*, Phys. Rev. D **73** (2006) 123526 [astro-ph/0512159].

[41] C. Gordon, K. Land and A. Slosar, *Cosmological Constraints from Type Ia Supernovae Peculiar Velocity Measurements*, Phys. Rev. Lett. **99** (2007) 081301 [arXiv:0705.1718 [astro-ph]].

[42] R. A. Vanderveld, E. E. Flanagan and I. Wasserman, *Mimicking dark energy with Lemaitre-Tolman-Bondi models: Weak central singularities and critical points*, Phys. Rev. D **74** (2006) 023506, [astro-ph/0602476].

[43] S. February, J. Larena, M. Smith and C. Clarkson, *Rendering dark energy void* Mon. Not. Roy. Astron. Soc. **405** (2010) 2231, [arXiv:0909.1479].

[44] G. R. Bengochea and M. E. De Rossi, *Dependence on supernovae light-curve processing in void models*, Phys. Lett. B **733** (2014) 258, [arXiv:1402.3167 [astro-ph.CO]].

[45] S. del Campo, I. Duran, R. Herrera and D. Pavon, *Three thermodynamically-based parameterizations of the deceleration parameter*, Phys. Rev. D **86** (2012) 083509 [arXiv:1209.3415 [gr-qc]].

[46] V. Sahni, A. Shafieloo and A. A. Starobinsky, *Model independent evidence for dark energy evolution from Baryon Acoustic Oscillations*, arXiv:1406.2209 [astro-ph.CO].

Data Set	$\chi^2_{min}/d.o.f.$	Ω_m	w_0	$w_1(w_{0.5})$
JBP parametrization				
Constitution	461.597/394	0.444 ± 0.048	-0.125 ± 0.647	-13.820 ± 8.510
C+BAO+CMB	467.778/403	0.284 ± 0.008	-0.929 ± 0.190	-0.649 ± 1.383
Union 2	541.338/554	0.414 ± 0.072	-0.769 ± 0.439	-7.201 ± 7.659
U2+BAO+CMB	544.752/563	0.283 ± 0.008	-1.051 ± 0.164	0.144 ± 1.173
Union 2.1	562.222/577	0.294 ± 0.262	-1.011 ± 0.199	-0.274 ± 5.717
U21+BAO+CMB	564.364/586	0.283 ± 0.008	-1.041 ± 0.156	0.118 ± 1.108
LOSS-Union	573.643/583	0.333 ± 0.099	-0.684 ± 0.289	-4.908 ± 5.503
LU+BAO+CMB	581.007/592	0.288 ± 0.009	-0.984 ± 0.162	-0.523 ± 1.275
FSLLI parametrization				
Constitution	461.099/394	0.452 ± 0.042	-0.280 ± 0.546	-9.472 ± 5.503
C+BAO+CMB	467.870/403	0.284 ± 0.008	-0.966 ± 0.138	-0.235 ± 0.616
Union 2	541.476/554	0.419 ± 0.069	-0.904 ± 0.348	-4.510 ± 4.989
U2+BAO+CMB	544.697/563	0.283 ± 0.008	-1.063 ± 0.124	0.141 ± 0.536
Union 2.1	562.208/577	0.230 ± 0.610	-0.965 ± 0.630	0.388 ± 3.294
U21+BAO+CMB	564.356/586	0.282 ± 0.008	-1.041 ± 0.119	0.071 ± 0.514
LOSS-Union	573.835/583	0.362 ± 0.084	-0.748 ± 0.265	-3.859 ± 3.982
LU+BAO+CMB	581.217/592	0.287 ± 0.009	-1.029 ± 0.118	-0.109 ± 0.580
FSLLII parametrization				
Constitution	459.922/394	0.461 ± 0.032	-0.703 ± 0.350	-36.447 ± 21.044
C+BAO+CMB	468.001/403	0.283 ± 0.008	-1.008 ± 0.069	-0.079 ± 0.461
Union 2	541.979/554	0.424 ± 0.061	-1.192 ± 0.188	-13.110 ± 16.789
U2+BAO+CMB	544.517/563	0.282 ± 0.008	-1.058 ± 0.066	0.199 ± 0.373
Union 2.1	562.205/577	0.239 ± 0.406	-0.942 ± 0.648	0.531 ± 3.581
U21+BAO+CMB	564.349/586	0.282 ± 0.008	-1.033 ± 0.065	0.065 ± 0.400
LOSS-Union	574.452/583	0.367 ± 0.088	-1.027 ± 0.129	-9.274 ± 13.042
LU+BAO+CMB	580.109/592	0.280 ± 0.008	-1.090 ± 0.055	0.371 ± 0.292
SL parametrization				
Constitution	460.998/394	0.453 ± 0.0408	-0.301 ± 0.542	-4.443 ± 1.930
C+BAO+CMB	467.949/403	0.284 ± 0.008	-0.992 ± 0.098	-1.034 ± 0.072
Union 2	541.500/554	0.423 ± 0.066	-0.911 ± 0.352	-2.950 ± 1.933
U2+BAO+CMB	544.590/563	0.282 ± 0.008	-1.065 ± 0.087	-1.014 ± 0.055
Union 2.1	562.219/577	0.255 ± 0.417	-0.984 ± 0.464	-0.896 ± 1.574
U21+BAO+CMB	564.351/586	0.282 ± 0.008	-1.036 ± 0.086	-1.019 ± 0.059
LOSS-Union	573.840/583	0.353 ± 0.089	-0.806 ± 0.229	-2.198 ± 1.417
LU+BAO+CMB	580.632/592	0.281 ± 0.009	-1.099 ± 0.075	-1.013 ± 0.053
BA parametrization				
Constitution	460.793/394	0.456±0.038	-0.363±0.508	-7.596±4.371
C+BAO+CMB	467.895/403	0.282±0.008	-1.006±0.095	0.006±0.243
Union 2	541.576/554	0.422±0.062	-0.974±0.301	-3.460±3.720
U2+BAO+CMB	544.570/563	0.281±0.008	-1.075±0.088	0.163±0.209
Union 2.1	562.187/577	0.143±1.185	-0.850±1.294	0.407±1.302
U21+BAO+CMB	564.274/586	0.281±0.008	-1.047±0.086	0.103±0.210
LOSS-Union	573.933/583	0.356±0.088	-0.848±0.206	-2.442±2.865
LU+BAO+CMB	581.294/592	0.280±0.008	-1.105±0.075	0.215±0.187

Table 1. Best fits for the free parameters using several data sets for the parametrizations of the EoS of dark energy.